UC Irvine

UC Irvine Previously Published Works

Title

Rapid submarine melting of the calving faces of west Greenland tidewater glaciers

Permalink

https://escholarship.org/uc/item/9kf0p0rw

Journal

Nature Geosc, 3(3)

ISSN

1752-0908

Authors

Rignot, E

Koppes, M

Velicogna, I

Publication Date

2010

Copyright Information

This work is made available under the terms of a Creative Commons Attribution License, available at https://creativecommons.org/licenses/by/4.0/

Peer reviewed

eScholarship.org Powered by the California Digital Library
University of California

nature geoscience

LETTERS

PUBLISHED ONLINE: 14 FEBRUARY 2010 | DOI: 10.1038/NGEO765

Rapid submarine melting of the calving faces of West Greenland glaciers

Eric Rignot[1,2]*, Michele Koppes[3] and Isabella Velicogna[1,2]

Widespread glacier acceleration has been observed in Greenland in the past few years[1–4] associated with the thinning of the lower reaches of the glaciers as they terminate in the ocean[5–7]. These glaciers thin both at the surface, from warm air temperatures, and along their submerged faces in contact with warm ocean waters[8]. Little is known about the rates of submarine melting[9–11] and how they may affect glacier dynamics. Here we present measurements of ocean currents, temperature and salinity near the calving fronts of the Eqip Sermia, Kangilerngata Sermia, Sermeq Kujatdleq and Sermeq Avangnardleq glaciers in central West Greenland, as well as ice-front bathymetry and geographical positions. We calculate water-mass and heat budgets that reveal summer submarine melt rates ranging from 0.7 ± 0.2 to 3.9 ± 0.8 m d^{-1}. These rates of submarine melting are two orders of magnitude larger than surface melt rates, but comparable to rates of iceberg discharge. We conclude that ocean waters melt a considerable, but highly variable, fraction of the calving fronts of glaciers before they disintegrate into icebergs, and suggest that submarine melting must have a profound influence on grounding-line stability and ice-flow dynamics.

In the past decade, surface melt around Greenland has markedly increased in magnitude and spatial extent, whereas snowfall has increased only slightly[12–14]. As a result, the ice-sheet mass deficit tripled in the period 1996–2007 (ref. 15). Critically, 50–60% of that loss was caused by an acceleration of the outlet glaciers; the remainder resulting from an increase in surface melt. Hence, glacier acceleration is a significant, if not dominant, response to climate warming.

The widespread two- to threefold acceleration of the glaciers cannot be explained solely by enhanced lubrication of the bed from surface meltwater[16], for seasonal variations in glacier velocity do not exceed 8–10%, independent of latitude[1]. Glacier acceleration is instead probably caused by the ungrounding of ice fronts from the bed, which reduces buttressing of inland ice and entrains faster rates of ice flow to the ocean[5]. To unground glaciers from the bed, they must melt and thin. Warmer air temperatures thin the glaciers from the surface and allow the ice flotation margin to migrate inland. Such surface melting is well documented in Greenland[12–14]. However, melting can also occur along the submarine termini of the glaciers. A warmer ocean will erode submerged grounded ice and cause the grounding line to retreat. In contrast, we know very little about rates of submarine melting along calving fronts. The only measurements of submarine glacier melting so far have been conducted in Alaska[9,10].

In August 2008, we deployed two InterOcean S4 conductivity, temperature and depth (CTD)/current meters, a Seabird SBE-19 conductivity and temperature density profiler, and a Lowrance 18C sonar depth sounder with a global positioning system in the fjords of Eqip Sermia (EQIP), Kangilerngata Sermia (KANGIL) and Sermeq Kujatdleq and Avangnardleq (TOR), 100 km north of Ilulissat (Fig. 1). Seven to ten casts were taken at 500–1,000 m intervals in each fjord, between 200 and 1,000 m (EQIP and KANGIL) and 4 km (TOR) from the ice fronts. We sampled the water column from 1 m below the surface to a depth of 80 m at EQIP, 150 m at KANGIL and 200 m at TOR, which is not the entire water column. Water velocity, temperature and salinity were measured continuously, as well as averaged, at 1.5-m depth intervals in the top 50 m and at 15-m intervals below 50 m, because most of the velocity structure was observed in the upper layers[9,11]. Fjord bathymetry was also mapped, except in TOR where the fjord depth exceeded our instrument capability. We complemented our bathymetric data with a global bathymetric data set[17], which agreed to within 10–15 m at the fjord centres with our measurements, but differed by up to 80 m along the fjord edges because of poor definition of the land–ocean boundary in the global data set. During the survey, we experienced mildly warm weather (5–15 °C), calm wind conditions and no remnant seasonal sea-ice.

To model the forced convective flow into the fjord and derive its mass and heat budgets, we modified the method of Motyka and colleagues[9]. In this two-layer approach, subglacial water discharge drives ocean convection, drawing deep, warm saline waters towards the near-vertical terminal ice face, where the two components turbulently mix and rise along the face to reach the surface and flow away from the terminus in an overflow plume (Fig. 2). The ascending waters melt ice along the calving face, and contribute to the overflow plume. Subglacial meltwater typically rises to the water surface within a kilometre of the ice front[11]. The overflow plume is not necessarily homogeneous, because subglacial water is ejected at discrete locations across the glacier front. Greenland's fjords are also fronted by shallow sills that limit the exchange of warm, saline water between the ocean and the fjord. EQIP and KANGIL have sill depths of 200 m. TOR is 450 m deep near the ice front, with a sill depth of 300 m at the fjord entrance[17].

The casts revealed the presence of small jets in the upper 40–60 m of the water column (Fig. 3). Salinity and temperature increase with depth, except at EQIP where the unstratified temperature data suggest an inflow of warm water to the glacier centre and an outflow of colder water along the fjord sides. In EQIP, jets at 10 and 30 m depth flow at 30–35 cm s^{-1} away from the ice to the northwest, along the deepest trough (Figs 1 and 3). With inflow coming from the south to the glacier centre, this circulation pattern is contrary to that observed in the other fjords and to our simplified model. Below 50 m depth, however, current speeds drop to a few centimetres per second, agreeing with a two-layer structure. In KANGIL, high outflow is observed above 40 m depth along the western and eastern edges of the fjord. In TOR, similar jets are found in the top 60 m to the north and

[1]University of California, Earth System Science, Irvine, California 92617, USA, [2]Jet Propulsion Laboratory, Pasadena, California 91109, USA, [3]University of British Columbia, Department of Geography, Vancouver, British Columbia, V6T 1Z2, Canada. *e-mail: erignot@uci.edu.

© 2010 Macmillan Publishers Limited. All rights reserved.

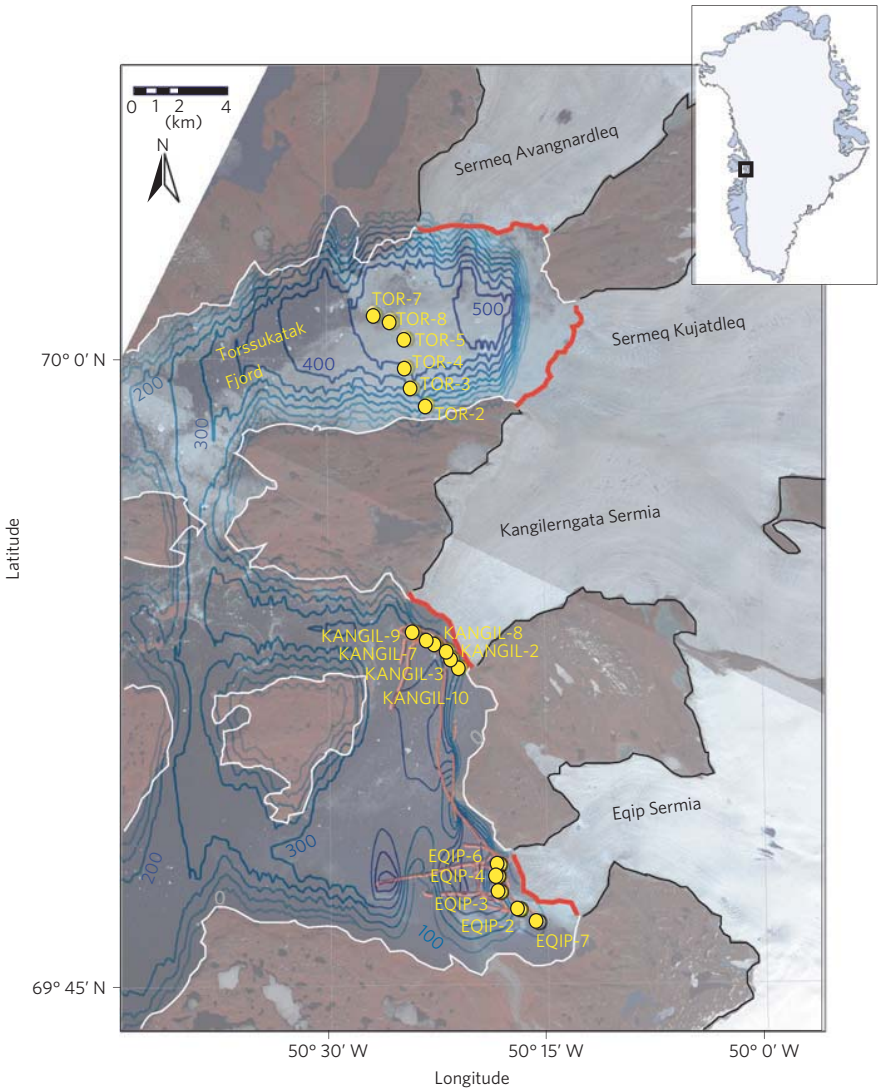

Figure 1 | Bathymetry and location of study area. Bathymetric contours (50-m interval, blue lines) and cast locations (yellow dots with cast names) for Eqip Sermia, Kangilerngata Sermia, Sermeq Kujatdleq and Sermeq Avangnardleq, West Greenland, overlaid on an ASTER satellite image. Bathymetric survey lines are thin red lines. Ocean–ice, land–ice and land–ocean boundaries are, respectively, delineated as thick red, thin black and thin white lines. The black square in the inset map shows the location of the glaciers in central West Greenland.

middle of the fjord, all drawing water away from the glacier front. In all three fjords, we had no visual evidence of upwelling of turbid subglacial waters in front of the glaciers, although these areas were covered in brash ice periodically stirred by the calving of icebergs.

To evaluate the errors in the simplified two-layer model, we considered both the uncertainty in the positioning of the transition boundary and uncertainties in the average temperature and salinity of the inflow layer (see the Methods section). All calculations assume steady-state conditions and negligible influence of tidal currents. As the flow pattern in EQIP calls our simplified model into question, we also calculated the mass and heat budget of the entire water column in EQIP and KANGIL fjords. The results from the two approaches agreed quite well (within 2–20%), which provides a verification of our model.

In EQIP, the calculated freshwater outflux of $116 \pm 11\ m^3\ s^{-1}$ is 3% of the incoming flux of $3{,}362 \pm 278\ m^3\ s^{-1}$. The heat budget indicates a submarine meltwater production of $5 \pm 2\ m^3\ s^{-1}$ for a net submarine melt rate of $0.7 \pm 0.2\ m\ d^{-1}$ across the 0.6-km^2 submerged ice face. In KANGIL, the freshwater outflux is $286 \pm 61\ m^3\ s^{-1}$ with a submarine melt flux of $18 \pm 4\ m^3\ s^{-1}$.

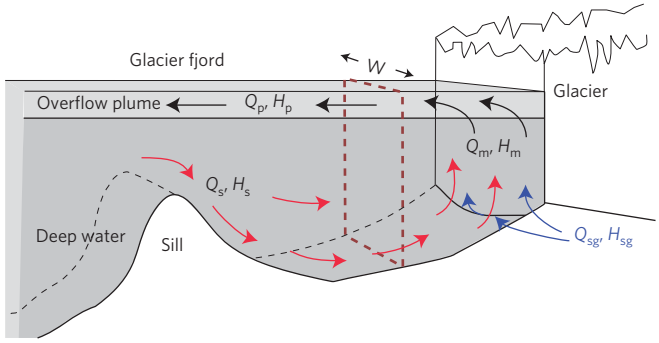

Figure 2 | A simplified two-layer model of forced convective flow in a glacier fjord. Deep-water access is guarded by a sill and terminated by a calving front[9]. The incoming mass flux from the deep ocean, Q_s, and from subglacial water, Q_{sg}, is balanced by the mass flux from the overflow plume, Q_p, and the submarine meltwater, Q_m. The incoming deep-ocean heat flux, H_s, and subglacial water heat flux, H_{sg}, melt submarine ice with a heat flux, H_m, to yield an overflow plume with a heat flux, H_p. The overflow plume is not homogeneous in velocity structure.

© 2010 Macmillan Publishers Limited. All rights reserved.

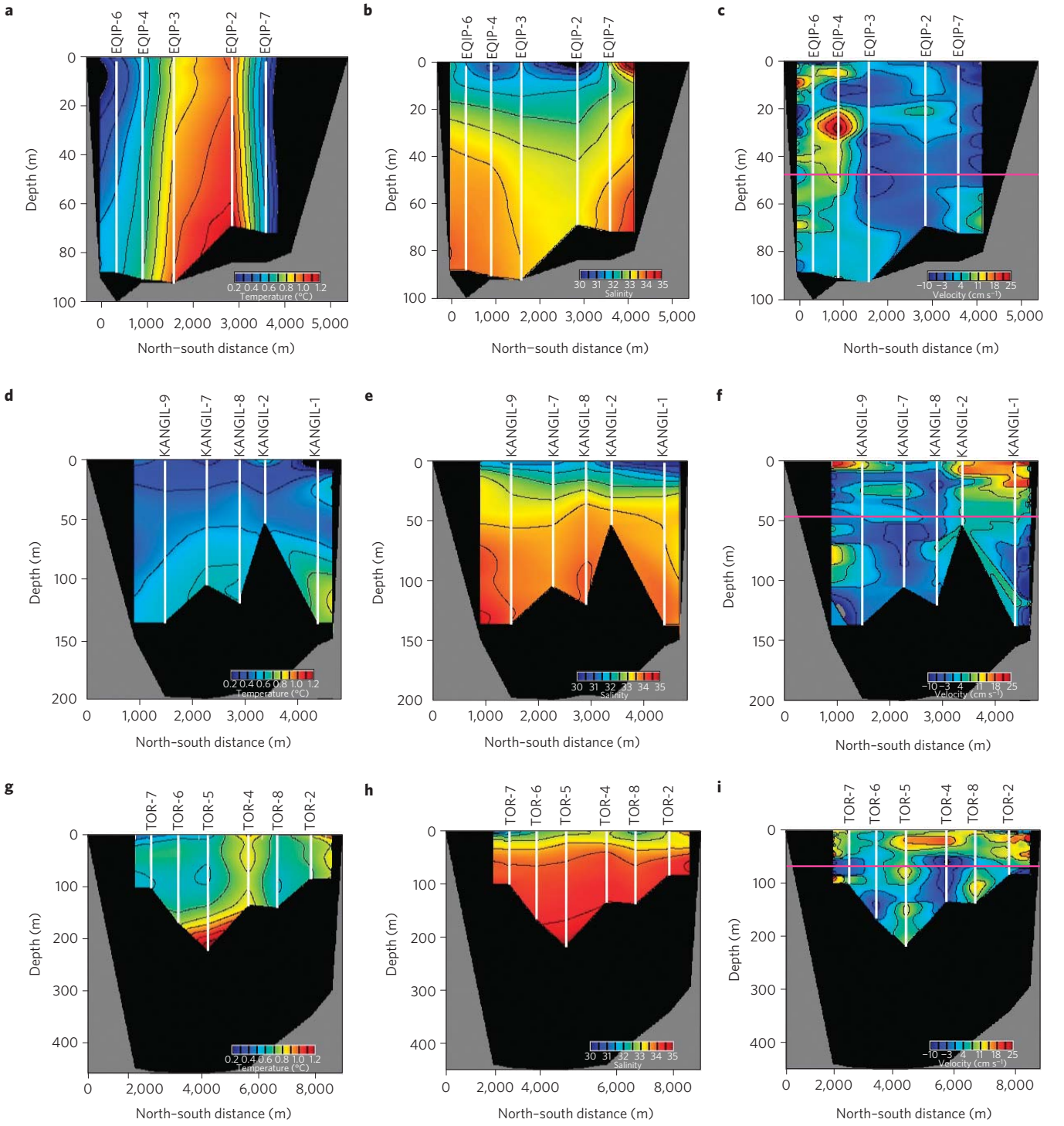

Figure 3 | Water characteristics in three West Greenland glacial fjords. a–i, Water temperature (°C), salinity and velocity normal to the flux gate (cm s^{-1}, positive outward, negative towards the glacier front) for EQIP (**a–c**), KANGIL (**d–f**) and TOR (**g–i**) as a function of water depth (m) and distance from north to south (m). The position of individual casts is noted as a white vertical line. The purple horizontal lines at 47 m (EQIP, KANGIL) and 57 m (TOR) depth denote the transition boundary between the overflow plume and the deeper ocean inflow used in our calculations. The horizontal and vertical scales vary from one glacier plot to the next. Water-column areas with no data are coloured black. Areas with no ocean water (that is, at the edges of the fjord) are coloured grey.

The average melt rate across the 0.6-km^2 submerged area is 2.6 ± 0.5 m d^{-1}. In TOR, the freshwater outflux of 874 ± 46 m^3 s^{-1} is 3% of the mass inflow. The submarine melt flux of 255 ± 33 m^3 s^{-1} is 30% of the freshwater outflux and yields a submarine melt rate of 3.9 ± 0.8 m d^{-1} across the 5.7-km^2 submerged area of the two ice fronts. Ocean thermal forcing, that is, the difference between the water temperature and the freezing point of sea water at the base of the calving face, is 2.8, 3.0 and 3.8 °C, respectively, for the three fjords.

Ice–ocean interaction models suggest that submarine melting increases with the square of thermal forcing from the ocean[18]. At Leconte Glacier, summer submarine melting was 12 m d^{-1} (ref. 9)

© 2010 Macmillan Publishers Limited. All rights reserved.

Table 1 | Mass and heat budgets of three West Greenland glacial fjords from a two-layer model.

Fjord	EQIP	KANGIL	TOR
Q_s	3,362±278	5,521±394	26,967±1,000
Q_p	3,478±280	5,807±409	27,841±1,018
Q_{sg}	111±10	268±60	619±33
Q_m	5±2	18±4	255±33
H_s	7.6±0.5	15.7±0.2	160.6±14
H_p	5.9±0.2	9.4±0.8	74.8±3
H_m	1.7±0.3	6.3±0.9	85.8±14
V_m	0.7±0.2	2.6±0.5	3.9±0.8
Q_r	132±65	160±76	516±236
Q_f	25±5	24±4	338±15

Water influx from the deep ocean, Q_s, outfluxes from the overflow plume, Q_p, the subglacial water, Q_{sg}, and the submarine meltwater, Q_m, in cubic metres per second. Heat influx from the ocean, H_s, and outfluxes from the overflow plume, H_p, and to melt submarine ice, H_m in 10^9 watts. Submarine melt rate, V_m, in metres per day. July–August 2008 average runoff production, Q_r, and ice-front discharge, Q_f, in cubic metres per second of water equivalent. The submerged areas of the three glaciers are 0.612 km^2, 0.626 km^2 and 5.68 km^2 (see Supplementary Information). The full water-column budget calculation at EQIP yields $Q_{sg} = 118 \pm 10\ m^3\ s^{-1}$, $Q_m = 4 \pm 2\ m^3\ s^{-1}$, $H_m = 1.3 \pm 0.3 \times 10^9$ W and $V_m = 0.6 \pm 0.2\ m\ d^{-1}$. At KANGIL, we find $Q_{sg} = 297 \pm 60\ m^3\ s^{-1}$, $Q_m = 18 \pm 4\ m^3\ s^{-1}$, $H_m = 6.2 \pm 0.8 \times 10^9$ W and $V_m = 2.6 \pm 0.5\ m\ d^{-1}$.

with a thermal forcing of 7.3 °C. This would imply rates of 1.8, 2.0 and 3.2 m d^{-1} for EQIP, KANGIL and TOR fjords based on similar thermal forcing, which is reasonably close to our calculations. Similarly, submarine melting depends on the sine of the basal slope of the ice face[18]. Beneath floating ice shelves, melt rates range from centimetres to tens of metres per year[19], but the sine of their basal slope is typically only 0.01–0.02, two orders of magnitude lower than for the vertical faces of tidewater glaciers, where much larger melt rates are expected.

The average July–August 2008 runoff at the three glaciers[12,14] is estimated at 132 ± 65, 160 ± 76 and $516 \pm 236\ m^3\ s^{-1}$ versus calculated subglacial water fluxes of 111 ± 10, 267 ± 60 and $619 \pm 33\ m^3\ s^{-1}$ (Table 1). This agreement within error bars of the two estimates provides an independent validation of our water budget calculations. We also calculated ice-front discharge in water equivalent using a standard approach[15] to obtain 25 ± 5, 24 ± 4 and $338 \pm 15\ m^3\ s^{-1}$, respectively, versus submarine meltwater fluxes of 5 ± 2, 18 ± 4 and $255 \pm 33\ m^3\ s^{-1}$ (Table 1). We conclude from this comparison that 20–80% of the summer ice-front fluxes are directly melted by the ocean. Submarine melting is therefore a major form of ice ablation, which also varies significantly from one fjord to the next.

In winter, subglacial water discharge will decrease because runoff production ceases, forced convection in front of the glacier will slow down and submarine melting will decrease. This has been observed at Columbia Glacier[10]. Our summer submarine melt rates are therefore unlikely to be representative of year-round melt rates, and the importance of submarine melting in the mass budget may be reduced in winter.

Surface melt rates in the lower 5 km of the three glacier systems averaged 4–18 cm d^{-1} in July–August 2008 (highest value in July; refs 12, 14). Our inferred submarine melting rates are two orders of magnitude larger. Submarine melting is therefore a major ablation process across tidewater glacier fronts. This has several important consequences for glacier dynamics. First, submarine melting is more likely to dislodge glaciers from their beds than surface melting. Enhanced submarine melting, either from warmer ocean waters or enhanced forced convection by increased subglacial discharge, will melt grounded ice directly and cause grounding-line retreat. Our data show that a thermal forcing of 3 °C melts ice at a rate of several metres per day, that is, hundreds of metres in one summer. In comparison, an increase in surface melting will be effective at ungrounding a glacier only if the glacier surface slope is low so that the line of hydrostatic equilibrium retreats rapidly with a small change in ice thickness. Furthermore, if the glacier retreats into deeper waters, submarine melting will increase because the submerged area and the pressure-dependent melting point of ice will both increase, two positive feedbacks. Moreover, submarine melting must have an enormous influence on ice calving mechanics. Pronounced submarine melting will undercut the submerged ice faces and promote calving from below the water surface, a mode of calving frequently observed at tidewater termini[9,20]. In winter, reduced submarine melting may explain the reduced iceberg production noted at many outlet glaciers[21].

It was recently suggested that a warming of Greenland's fjord waters in the late 1990s may have triggered glacier acceleration[8]. For Jakobshavn Isbrae, previous studies of ice-shelf melting suggest that a 3 °C increase in ocean temperature would increase submarine melting by 30–70 m yr^{-1} (ref. 19), which is large enough to explain the observed ice-shelf disintegration. For tidewater glaciers in southeast Greenland, a 3 °C thermal forcing could increase submarine melting to rates comparable to those calculated herein, that is, hundreds of meters in one summer, with considerable spatial variability. Such retreat rates could destabilize the glaciers rapidly. In Greenland, tidewater glaciers control 90% of the ice discharge into the ocean. Submarine melting may therefore have a large indirect impact on the entire ice-sheet mass budget. If we are to determine the future of the Greenland ice sheet more reliably, it is essential to document these ice–ocean interactions more completely and in greater detail.

Methods

Current velocities were averaged over 5 min at each depth interval to obtain stable solutions. Ocean current measurements were corrected for boat drift calculated from the global positioning system data. We did not correct for tidal currents, but we estimate them to be low in this area. Using the Arctic Ocean barotropic model (AOTIM-5; ref. 22), we calculate tides of ±60 cm and tidal currents of ±3 cm s^{-1} during our time period (8–11 August 2008) at 70° N, 50.5° W. Noise in our velocity data is ±2 cm s^{-1}.

Vertical profiles of temperature and salinity were collected continuously both during descent and ascent of the instruments. Comparison of one S4 CTD with the calibrated SBE-19 CTD on one cast (we subsequently lost the SBE-19 CTD to iceberg impingement) showed an excellent agreement in temperature and salinity for the data retrieved during ascent. The agreement was poorer during descent because the S4 CTDs took longer to stabilize after entering the water. The S4 CTDs, which were deployed in parallel, were subsequently cross-calibrated and absolutely calibrated to match the SBE-19 measurements. Measurements disturbed by boat motion from a calving event or human intervention were discarded. The S4 probes experienced difficulties in the presence of extensive amounts of brash ice; in such instances, casts were repeated until stable solutions were obtained. The precision in temperature is 0.05 °C and salinity is 0.1.

Errors associated with temporal changes in ocean current, salinity and temperature measurements are difficult to estimate because our survey was limited to one week. We re-occupied KANGIL-1, EQIP-2 and EQIP-3 three days apart and obtained temperature and salinity within error bars and mass and heat budgets not significantly different from the previous calculations, hence providing indirect support for our steady-state assumption.

The errors in mass and heat budget are quoted in Table 1. We varied the position of the transition boundary between the overflow plume and ocean inflow in 5-m increments by ±10 m, averaged the results and calculated the standard deviation. The depth of the boundary was determined to be 47 ± 10 m in EQIP, 47 ± 10 m in KANGIL and 57 ± 10 m in TOR. Another source of error is in the selection of a mean temperature and salinity for the deep ocean. We extrapolated our data to the sea bed using a linear scheme to calculate the depth-averaged temperature and salinity of the ocean below the transition boundary. We compared these values with those measured midway in the lower section to quantify the uncertainty in temperature and salinity. The uncertainty associated with salinity is small. In TOR, only one cast was deep enough to cover the midway point, so we assumed the same thermal forcing on all casts, with an uncertainty of ±0.1 °C. The errors in boundary position and mean temperature were treated as independent errors when calculating the total error.

Errors of omission may be significant because part of the outflow may have exceeded the edges of our survey, yet the sea bed is also shallower along the fjord sides. We did not include this error source in our estimates.

© 2010 Macmillan Publishers Limited. All rights reserved.

Received 10 September 2009; accepted 5 January 2010; published online 14 February 2010

References

1. Rignot, E. & Kanagaratnam, P. Changes in the velocity structure of the Greenland Ice Sheet. *Science* **311,** 986–990 (2006).
2. Howat, I., Joughin, I. & Scambos, T. Rapid changes in ice discharge from Greenland outlet glaciers. *Science* **315,** 1559–1561 (2007).
3. Luckman, A., Murray, T., de Lange, R. & Hanna, E. Rapid and synchronous ice-dynamic changes in East Greenland. *Geophys. Res. Lett.* **33,** L03503 (2006).
4. Joughin, I., Abdalati, W. & Fahnestock, M. Large fluctuations in speed on Greenland's Jakobshavn Isbrae glacier. *Nature* **432,** 608–610 (2004).
5. Thomas, R. H. Force-perturbation analysis of recent thinning and acceleration of Jakobshavn Isbrae. *Greenland J. Glaciol.* **50,** 57–66 (2004).
6. Thomas, R. H., Rignot, E., Kanagaratnam, P., Krabill, W. & Casassa, G. Force-perturbation analysis of Pine Island Glacier, Antarctica, suggests cause for recent acceleration. *Ann. Glaciol.* **39,** 133–138 (2004).
7. Howat, I., Joughin, I., Tulaczyk, S. & Gogineni, S. Rapid retreat and acceleration of Helheim Glacier, East Greenland. *Geophys. Res. Lett.* **32,** L22502 (2005).
8. Holland, D., Thomas, R. H., de Young, B. & Ribergaard, M. H. Acceleration of Jakobshavn Isbrae triggered by warm subsurface ocean waters. *Nature Geosci.* **1,** 659–664 (2008).
9. Motyka, R., Hunter, L., Echelmeyer, K. & Connor, C. Submarine melting at the terminus of a temperate tidewater glacier, Leconte Glacier, Alaska, USA. *Ann. Glaciol.* **36,** 57–65 (2003).
10. Walters, R., Josberger, E. G. & Driedger, C. L. Columbia Bay, Alaska: An upside down estuary. Estuarine, Coastal and Shelf. *Science* **26,** 607–617 (1988).
11. Horne, E. P. Ice-induced vertical circulation in an Arctic fjord. *J. Geophys. Res.* **90,** 1078–1086 (1985).
12. Box, J. *et al.* Greenland Ice Sheet surface mass balance variability (1988–2004) from calibrated polar MM5 output. *J. Clim.* **19,** 2783–2800 (2006).
13. Hanna, E. *et al.* Increased runoff from melt from the Greenland Ice Sheet: A response to global warming. *J. Clim.* **21,** 331–341 (2008).
14. Ettema, J. *et al.* Higher surface mass balance of the Greenland ice sheet revealed by high-resolution climate modelling. *Geophys. Res. Lett.* **36,** L12501 (2009).
15. Rignot, E., Box, J. E., Burgess, E. & Hanna, E. Mass balance of the Greenland Ice Sheet from 1958 to 2007. *Geophys. Res. Lett.* **35,** L20502 (2008).
16. Joughin, I. *et al.* Seasonal speedup along the western flank of the Greenland Ice Sheet. *Science* **320,** 781–783 (2008).
17. Smith, W. H. F. & Sandwell, D. Global seafloor topography from satellite altimetry and ship depth soundings. *Science* **277,** 1957–1962 (1997).
18. Holland, P., Jenkins, A. & Holland, D. The response of ice shelf basal melting to variations in ocean temperature. *J. Clim.* **21,** 2558–2572 (2008).
19. Rignot, E. & Jacobs, S. S. Rapid bottom melting widespread near Antarctic Ice Sheet grounding lines. *Science* **296,** 2020–2023 (2002).
20. Warren, C. R. Terminal environment, topographic control and fluctuations of West Greenland glaciers. *Boreas* **20,** 1–15 (1991).
21. Sohn, H. G., Jezek, K. & van der Veen, C. Jakobshavn Glacier, West Greenland: 30 years of spaceborne observations. *Geophys. Res. Lett.* **25,** 2699–2702 (1998).
22. Padman, L. & Erofeeva, S. A barotopic inverse tidal model for the Arctic Ocean. *Geophys. Res. Lett.* **31,** L02303 (2004).

Acknowledgements

This work was carried out at the Earth System Science Department of Physical Sciences, University of California, Irvine and at the California Institute of Technology's Jet Propulsion Laboratory under a contract with the National Aeronautics and Space Administration's Cryospheric Science Program. We thank B. Hallet, K. Steffen, E. Domack and S. Tulacyk for their generous loan of oceanographic equipment used, and J. Box and J. Ettema for providing estimates of summer 2008 runoff.

Author contributions

All authors discussed the results and commented on the manuscript. E.R. led the analysis, development of the paper and integration of the results with other data. M.K. analysed the ocean data and the ice-front bathymetry. I.V. helped collect and analyse the ocean data.

Additional information

The authors declare no competing financial interests. Supplementary information accompanies this paper on www.nature.com/naturegeoscience. Reprints and permissions information is available online at http://npg.nature.com/reprintsandpermissions. Correspondence and requests for materials should be addressed to E.R.

© 2010 Macmillan Publishers Limited. All rights reserved.